TGF-β1 alters microRNA profile in human gastric cancer cells

Haiyan Zhou, Kuansong Wang, Zhongliang Hu, Jifang Wen

Department of Pathology, Xiang-ya School of Medicine, Central South University, Changsha 410013, China
Corresponding to: Jifang Wen. Department of Pathology, Xiang-ya School of Medicine, Central South University, Changsha 410013, China.
Email: jifangwen@hotmail.com.

Objective: MicroRNAs (miRNAs) are important regulators that play a key role in tumorigenesis and tumor progression. Transforming growth factor-β1 (TGF-β1) is involved in invasion and metastasis in many tumors. In this study, we investigated the microRNAs (miRNA) profiles altered by TGF-β1 in gastric cancer (GC) cells.

Methods: We detected the expression profiles of miRNA by miRNA microarray and quantitative real-time polymerase chain reaction. Migration and invasion, wound-healing assay, prediction of miRNA targets, Western blot and qRT-PCR analysis were carried out to determine the role of one selected miRNA, namely miR-193b, in affecting the biological behaviors of GC BGC823 cells.

Results: Among 847 human miRNAs in the microarray, three miRNAs (miR-27a, miR-29b-1 and miR-194) were up-regulated and three (miR-574-3p, miR-193b and miR-130b) were down-regulated in BGC823 cells treated with TGF-β1 compared with control. miR-193b suppressed the invasion and metastasis of GC cells *in vivo* and *in vitro*, and down-regulated urokinase-type plasminogen activator (uPA) protein in GC cells.

Conclusions: TGF-β1 altered miRNA expression profile in BGC823 cells. Among the altered miRNAs, TGF-β1 induced the down-regulation of miR-193b, which inhibited cell invasion and metastasis *in vivo* and *in vitro*, and down-regulated uPA protein in GC cells.

Key Words: TGF-β1 (transforming growth factor-β1); gastric cancer (GC); miRNA (microRNAs); expression

Introduction

Gastric cancer (GC) is the most common gastrointestinal malignancy in East Asia, Eastern Europe, and parts of Central and South America, and is the second leading cause of cancer-related deaths (1). Local invasion and distant metastasis are leading causes for the dismal outcome of GC patients. Mechanisms associated with GC have attracted numerous research attentions.

MicroRNAs (miRNAs) are a class of small (18-24 nucleotides), endogenous and non-coding RNAs that bind to the 3'-untranslated region (3'-UTR) of the target mRNAs so as to regulate protein expression by repressing translation or by promoting degradation of the target mRNA, or by enhancing translation at the posttranscriptional level (2). Increasing evidences have indicated that miRNAs play a key role in various biological processes, including cell differentiation, proliferation, apoptosis, stress resistance, fat metabolism, tumorigenesis, and tumor metastasis (2-4).

Transforming growth factor-β1 (TGF-β1) is a member of the TGF-β super-family that controls proliferation, differentiation, embryonic development, angiogenesis, wound healing and other functions in various cell types (5,6). TGF-β1 is overexpressed in multiple tumors including GC compared with normal mucosa tissues. Its expression is positively correlated with infiltrating depth, lymph node metastasis and recurrence, and is negatively correlated with prognosis of GC patients (7,8). Our previous study indicated that TGF-β1 treatment could promote the high metastasis potential in GC cell lines BGC823 and SGC7901 (9). TGF-β1 and miRNAs could influence each other in the process of pathogenesis (10-12).

In this study, we investigated the effect of TGF-β1 on global miRNA expression profile in GC cell line BGC823.

We selected one significantly down-regulated miRNA, miR-193b, to explore its *in vitro* and *in vivo* roles in the invasion and metastasis of human GC cells. We further searched for miR-193b targets using bioinformatics analysis, quantitative reverse transcription-polymerase chain reaction (qRT-PCR) and Western blot analysis.

Materials and methods

Cell culture and TGF-β1 treatment

Human GC cell lines BGC-823 (poor differentiation), SGC7901 (moderate differentiation) and MKN28 (well differentiation) were purchased from Type Culture Collection of the Chinese Academy of Sciences (Shanghai, China). Cells were maintained in Dulbecco's Modified Eagle's Medium (DMEM, Gibco-Invitrogen, Switzerland) supplemented with 10% fetal bovine serum, 50 IU/mL penicillin and 50 μg/mL streptomycin. All cells were grown at 37 ℃ in a humidified atmosphere containing 5% CO_2. GC cell lines were rendered quiescing by 24 hrs exposure to serum-free DMEM, which can repress cellular synthetic materials and were stimulated with TGF-β1 (10 ng/mL) for 24 or 36 hrs.

miRNA microarray

miRNA microarrays were purchased from CapitalBio Corporation (Beijing, China), corresponding to Sanger miRNA database V11 (http://microrna.sanger.uk). miRNAs were enriched from total RNA-extracted cells with mirVana miRNA Isolation Kit (Ambion, Foster City, CA, USA) and were labeled with mirVana Array Labeling Kit (Ambion). For miRNA profile analysis, labeled miRNAs from BGC823 treated with TGF-β1 for 0 h (BGC823/0 h), 24 hrs (BGC823/24 hrs) and 36 hrs (BGC823/36 hrs) were hybridized on each miRNA microarray consisting of 46,228 probes from 71 species and covered 847 human miRNAs. Each sample was analyzed twice. Fluorescence scanning was detected using a double-channel laser scanner (LuxScan 10K/A; CapitalBio, China). The figure signals were transformed to digital signals by image analysis software (LuxScan3.0; CapitalBio). Raw data were normalized and analyzed by the significance analysis of microassays software (SAM, version 2.1; Stanford University, CA, USA) as described previously (13).

QRT-PCR for miRNA

QRT-PCR was used to validate the miRNA microarray

results. Total RNAs were extracted from BGC823/0 h cells and BGC823/24 hrs cells using Trizol reagent (Invitrogen) according to the manufacturer's protocol. Concentration and purity of total RNAs were measured using a biophotometer (Eppendorf, Germany). Reverse transcription was performed using NCode VILO miRNA cDNA Synthesis Kit (Invitrogen). Briefly, 1 μg total RNA, 4 μL 5× reaction mix, 2 μL 10× superscript enzyme mix and diethylpyrocarbonate (DEPC) treated water up to 20 μL were mixed. Reactions were incubated in a DNAEngine peltier Thermal cycler PTC-200 (Bio-Rad, USA) for 60 mins at 37 ℃, 5 min at 95 ℃, and then held at 4 ℃. All reverse transcriptase reactions, including no-template controls, were run in duplicate. Real-time PCR was performed using express SYBR GreenER miRNA qRT-PCR Kit (Invitrogen) on 7,500 real-time PCR system (ABI, USA). The r reaction mixtures (20 μL), containing 10 μL express SYBR GreenER qPCR SuperMix, 0.4 μL miRNA-specific forward primer (Genecopoeia, China), 0.4 μL universal qPCR Primer, 0.04 μL ROX reference dye, 2 μL cDNA, and 7.16 μL DEPC-treated water, were incubated at 50 ℃ for 2 mins and at 95 ℃ 2 mins, followed by 40 cycles of 95 ℃ for 15 s and 60 ℃ for 1 min. All quantitative PCR reactions, including no-template controls, were performed in triplicate. The relative expression ratios of miRNAs were determined with the crossing point as the cycle number. U6 was used as endogenous control for normalization.

siRNA transient transfection

siRNA duplex homologs of miR-193b mimics (193bM) and miR-193b inhibitors (193bI) were synthesized by Gene-Pharma Co. (Shanghai, China). siRNA duplexes of non-specific sequences were used as negative control (NC) and inhibitor negative control (INC). Non-transfected cells (M) were examined in parallel. All siRNAs (193bM, 193bI, NC, INC and M) were transfected using Lipofectamine 2000 reagent (Invitrogen) according to the manufacturer's protocol.

Wound-healing assay

Cells were plated and grown overnight to reach confluence in a six-well plate. Monolayers of cells were wounded by dragging a 10-μL pipette tip. Cells were washed to remove cellular debris and allowed to migrate for 72 hrs. Images were taken at 0 h and 72 hrs after wounding using an inverted microscope.

In vitro cell migration and invasion assay

Cell migration and invasion were measured by a 8 μm-pore polycarbonate membrane, Millicell Hanging Cell Culture Inserts, in a transwell apparatus (Millipore, USA), coated with or without ECL Cell Attachment Matrix (Millipore). BGC823 cells transfected with miRNA mimics or inhibitors were plated 12 h after transfection in serum-free medium (2×10^4 cells per transwell) and allowed to migrate toward a 10% fetal bovine serum gradient for 6 hrs (migration) or 24 hrs (invasion). Cells that remained on the top of the filter were removed by wiping with a cotton swab. Cells that migrated to the bottom surface of the insert were fixed in 100% methanol for 30 mins, stained in 0.1% crystal violet for 20 mins, rinsed in phosphate buffered saline (PBS) twice and examined microscopically. The number of migrated cells was determined by counting from five randomly selected microscopic fields at 200× magnification. All experiments were performed in triplicate.

In vivo metastasis assay

Forty-eight Balb/c nude mice aged 4-6 weeks were purchased from Shanghai Laboratory Animal Company (Shanghai, China) and were randomly divided into six groups (eight mice per group). Cancer cells (transfected with 193bM, 193bI, NC, INC and M) were detached and resuspended in PBS. Subsequently, 0.2 mL of suspension containing 2×10^6 cells was injected into the abdominal cavity of each animal. The mice were sacrificed after 4 weeks and the number of visible tumors in the liver surface was counted with the naked eye. Representative liver tumors were removed, fixed, embedded in paraffin, sectioned into 4 μm layers, and stained with hematoxylin-eosin for histological analysis. This study was approved by the Institutional Animal Care and Use Committee of Xiang-ya Medicine School, Central South University.

Bioinformatics analysis

Basic information of selected miRNAs was obtained from miRBase (http://www.mirbase.org/search.shtml) for further research. To investigate the significance of the selected miRNAs, we screened potential targets by using TargetScan 5.1 (http://www.targetscan.org/) and Pictar (http://pictar.mdc-berlin.de/), which identify miRNA binding sites, as well as genes co-regulated by miRNAs in a coordinated manner. We used Functional Annotation Bioinformatics Microarray Analysis Tools from CapitalBio Corporation (http://www.capitalbio.com/zh-hans/support/MAS) to classify the functions of the potential target genes predicted by both TargetScan 5.1 and Pictar.

Semi-quantitative RT-PCR

The cDNA templates were used for amplification of a selected potential target gene, urokinase-type plasminogen activator (uPA), and β-actin (endogenous control). PCR primers were: uPA sense 5'-GGGAGATGAAGTTTGAGGTGGA-3' and uPA antisense 5'-GCCTTGGAGGGAACAGACGAG-3', β-actin sense 5'-CCCAGCACAATGAAGATCAAGATCAT-3', and β-actin antisense 5'-ATCTGCTGGAAGGTGGACAGCGA-3' (Sangon, China). PCR cycles were as follows: initial denaturation at 94 ℃ for 3 min, followed by 30 cycles of 94 ℃ for 30 s, 59.8 ℃ for 30 s, 72 ℃ for 1 min, and final extension at 72 ℃ for 5 mins. PCR products were resolved on 1.5% agarose gels.

Western blot analysis

Cells were harvested and lysed in 100 μL WIP lysis buffer (Saichi, China). Equal amounts of protein extracted at the time after treatment were separated on 12% polyacrylamide and transferred to polyvinylidene difluoride (PVDF) membranes. The membranes were blocked in Tris-buffered saline containing Tween-20 [TBST; 0.2 mol/L NaCl, 10 mmol/L Tris (pH 7.4) and 0.2% Tween-20] with 3% bovine serum albumin (BSA; Sigma, USA) for 2 h at room temperature followed by incubation with primary antibodies in TBST at 4 ℃ overnight. Primary antibodies used for immunoblot analysis were anti-uPA (1:500; sc-14019, Santa Cruz, USA) and anti-GAPDH (1:500; CNM1002, Jiamay Biotech, China). Membranes were then washed three times with TBST followed by incubation with horseradish peroxidase-conjugated secondary antibody (1:2,000; 074-1807, Jiamay Biotech) in TBST at room temperature for 2 hrs. Bound antibody was detected using enhanced chemiluminescence (ECL; Pierce, USA).

Statistical analysis

Data were expressed as $\bar{x}\pm s$. The significance of differences between all groups was evaluated by using one-way analysis of variance (ANOVA) with a post hoc Student-Newman-Keuls multiple comparisons test. Statistical analyses were performed by using SPSS 13.0 Software (SPSS Inc., Chicago, IL, USA), and $P<0.05$ was considered as statistically significant.

Table 1 Signal ratio of 24 hrs to 0 h differentially expressed miRNAs of BGC823 cells after treated with TGF-β1

Differentially expressed miRNA	Signal ratio 24 h/0 h
miR-502-3p	0.493
miR-574-3p	0.556
miR-30a	0.566
miR-30c-2	0.588
miR-34b	0.598
miR-193a-5p	0.624
miR-140-3p	0.631
miR-193b	0.633
miR-532-5p	0.640
miR-130b	0.651
miR-455-3p	0.653
miR-27a	1.508
miR-138-1	1.513
miR-29b-1	1.520
miR-194	1.605
miR-93	1.765

Table 2 Signal ratio of 36 hrs to 0 h differentially expressed miRNAs of BGC823 cells after treated with TGF-β1

Differentially expressed miRNA	Signal ratio 36 h/0 h
miR-1308	0.431
miR-574-3p	0.510
miR-23a	0.560
miR-1275	0.580
miR-181b	0.584
miR-181c	0.589
miR-193b	0.599
let-7b	0.620
miR-130b	0.631
miR-92b	0.633
miR-1246	0.426
miR-212	1.500
miR-520c-5p	1.527
miR-29a	1.535
miR-301a	1.547
miR-224	1.573
miR-519c-5p	1.630
miR-27a	1.706
miR-29b-1	1.735
miR-192	2.001
miR-194	2.590

Results

miRNA profile alteration induced by TGF-β1 in BGC823 cells

The miRNA microarrays were used to analyze the miRNA profile alteration between BGC823/0 h, BGC823/24 hrs and BGC823/36 hrs cell lines treated with TGF-β1 (*Figure 1A*). We defined differentially expressed genes as no less than 1.5-fold change. There are 11 miRNAs down-regulated and 5 miRNAs up-regulated in BGC-823/24 hrs compared with BGC-823/0 h (*Table 1*). There are 11 miRNAs down-regulated and 10 miRNAs up-regulated in BGC-823/36 hrs compared with BGC-823/0 h (*Table 2*). The intersection of BGC-823/24 hrs and BGC-823/36 hrs consisted of six miRNAs (miR-574-3p, miR-193b and miR-130b down-regulated, miR-27a, miR-29b-1 and miR-194 up-regulated; *Table 3*). Three miRNAs (miR-193b, miR-130b and miR-27a) were selected for further investigation because which have the biggest differences in 24 and 36 hrs. In addition, from the *Table 1*, we knew that there is no different between 24 and 36 hrs for miR-193b. So, we just checked the qRT-PCR results at 0 and 24 hrs, respectively. qRT-PCR results revealed that miR-193b and miR-130b were down-regulated and miR-27a was up-regulated in BGC823 and SGC7901 cell lines (*Figure 1B,C*), which was

in accordance with miRNA microarray results. But these changes were not observed in MKN28 cell lines (*Figure 1D*).

miR-193b inhibits cell migration and invasion in vitro

To study the cellular function of miR-193b in GC, we transfected 193bM, 193bI or siRNA duplexes with non-specific sequences as NC and INC into BGC823 cells, respectively. miR-193b levels were effectively elevated by transfection of the mimics and were effectively decreased by transfection of the inhibitors (*Figure 2A*). In order to investigate the effect of miR-193b on BGC823 cell migration and invasion, an *in vitro* cell invasion assay was performed. Cells that migrated through the ECL Cell Attachment Matrix-coated membranes or non-coated membranes towards serum-containing medium were counted (*Figure 2B*). The inhibition of miR-193b significantly increased BGC823 cell migration compared with control (P<0.05). In addition, the over-expression of miR-193b significantly suppressed the migration and invasion of BGC823 cells through the filter
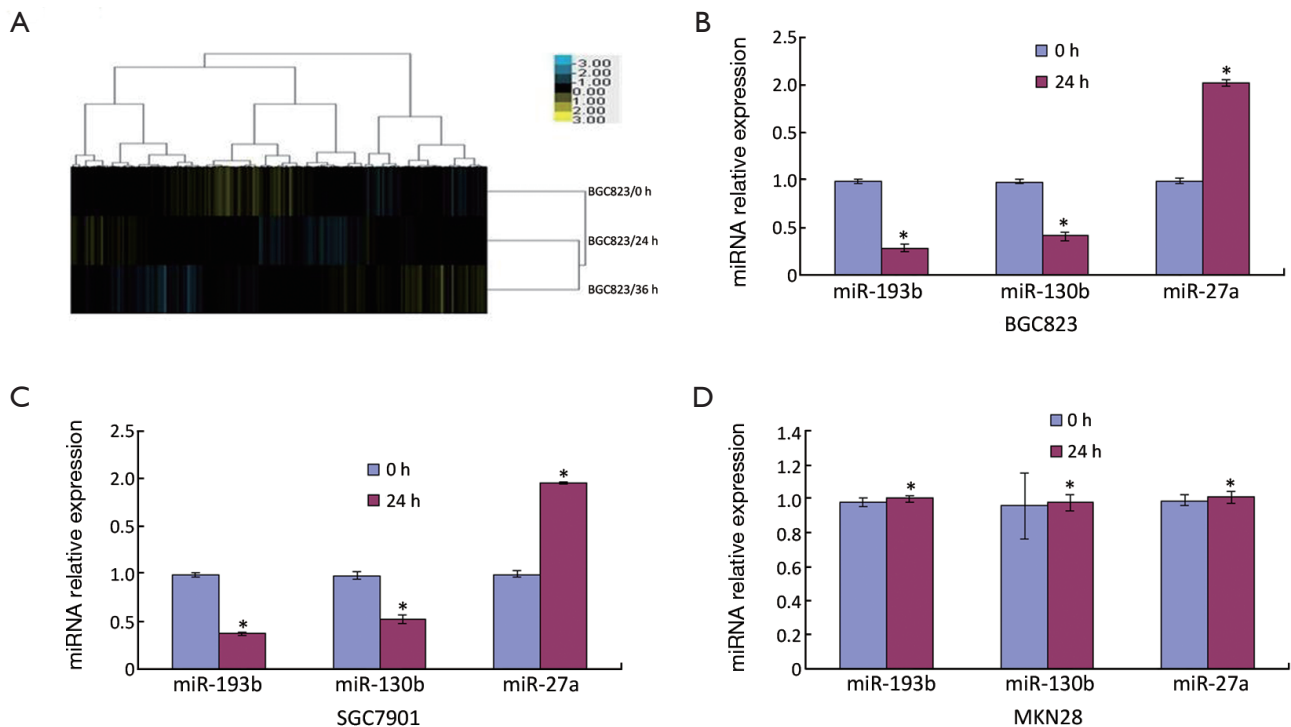
Figure 1 miRNA alternation induced by TGF-β1 treatment (n=3). A. The miRNA microarray clustering results of BGC823/0 h, BGC823/24 hrs and BGC823/36 hrs cell lines; B. qRT-PCR analysis of the relative expression levels of miR-193b, miR-130b and miR-27a in the same sample used for microarrays; C. qRT-PCR analysis of relative expression levels of miR-193b, miR-130b and miR-27a in SGC7901 cell lines; D. qRT-PCR analysis of relative expression levels of miR-193b, miR-130b and miR-27a in MKN28 cell lines. U6 RNA expression was used for normalization. *P<0.05

Table 3 The same differentially expressed miRNAs of BGC823 cells after treated with TGF-β 1 for 24 or 36 hrs

Differentially expressed miRNA	Signal ratio	
	24 h/0 h	36 h/0 h
miR-574-3p	0.556	0.510
miR-193b	0.633	0.599
miR-130b	0.651	0.631
miR-27a	1.508	1.706
miR-29b-1	1.520	1.735
miR-194	1.605	2.590

(P<0.05). Furthermore, the *in vitro* scratch wound-healing assay showed that miR-193b over-expression significantly suppressed BGC823 cell migration (P<0.05, *Figure 2C*), whereas miR-193b inhibition significantly increased cell wound repair (P<0.05, *Figure 2C*). Those results suggested that miR-193b is a regulator of migration and invasion in BGC823 cells.

miR-193b inhibits tumor invasion and metastasis in vivo

To address the potential effects of miR-193b on the *in vivo* invasion and metastasis of GC cells, equal numbers of BGC823 cells transfected with 193bM, 193bI, INC or NC respectively were injected into the abdominal cavity of nude mice. The number of metastatic nodi dramatically reduced in the nude mice group injected with the 193bM transfected cells compared with NC group (*Figure 3A*). The number of metastatic nodi increased in the group injected with the 193bI transfected cells compared to the INC group (*Figure 3B*). These results showed that miR-193b can inhibit tumor invasion and metastasis *in vivo*.

miR-193b targets prediction and bioinformatics analysis

Since miR-193b functioned as a tumor suppressor in GC, we further searched the potential targets of miR-193b by using web-based bioinformatics software. TargetScan and Pictar predicted 142 and 208 potential miR-193b targets,
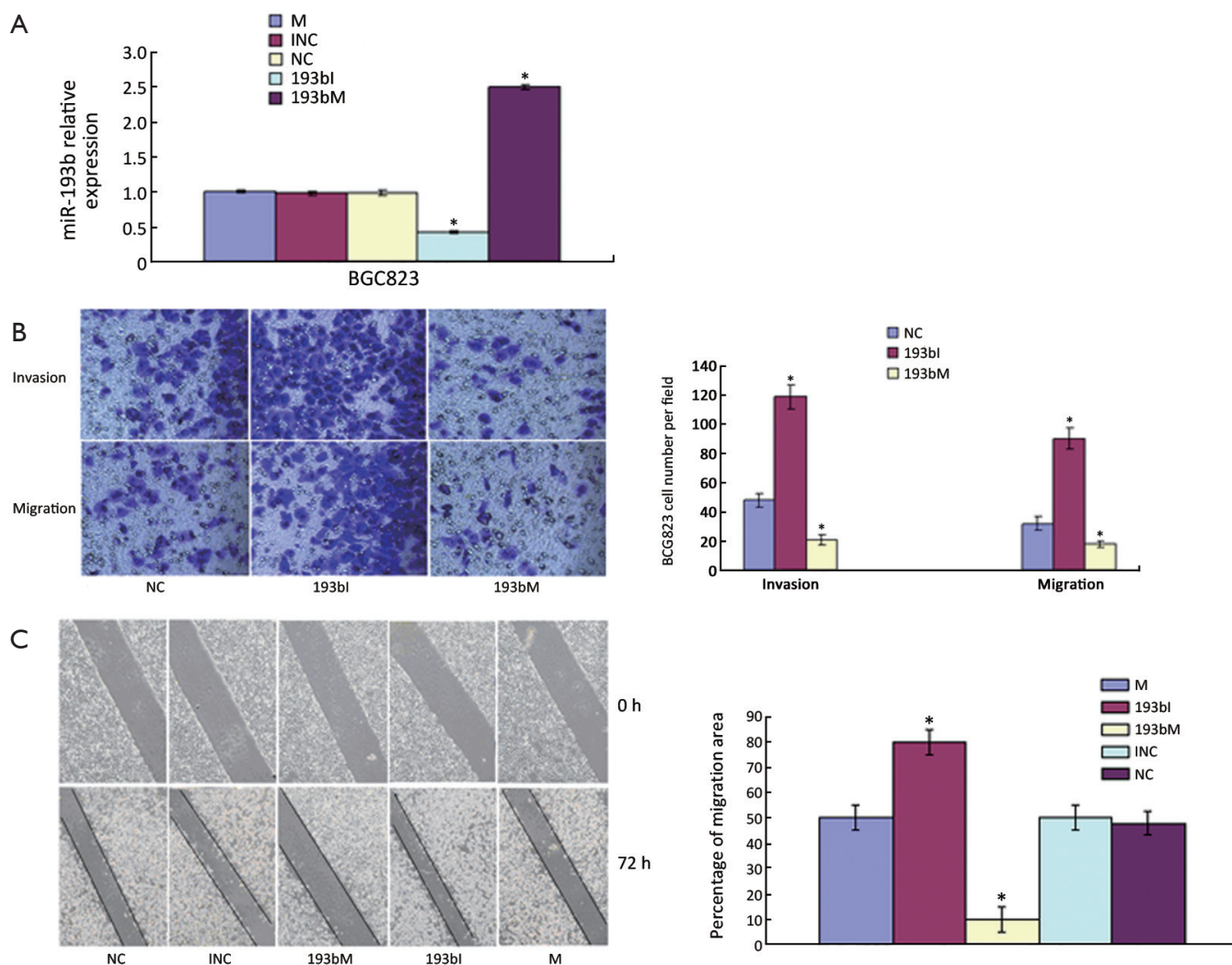
Figure 2 Effect of miR-193b on *in vitro* invasion and metastasis of BGC823 cells. A. Relative expression of miR-193b normalized to U6 in BGC823 cells after 193b inhibitor or mimics transient transfection measured by real-time PCR (n=3); B. *In vitro* invasion and migration assay. Representative fields of invasion and migration of BGC823 cells transfected with miR-193b-mimics or inhibitor on the membrane (left), (×200 magnification). The invasive or migration cell number of BGC823 cells transfected with miR-193b-mimics is drastically decreased than that transfected with negative control (n=10); C. Wound-healing assay. Left panel, representative images of BGC823 cells transfected with mimics or inhibitors at 0 and 72 hrs after wound scratch. Right panel, graphical presentation of the percentage of wound healing, which was counted as (0-72 hrs width of wound)/0 h width of wound (n=3). *P<0.05

respectively. To classify the functions of the potential targets, we used Functional Annotation Bioinformatics Microarray Analysis Tools and found that most targets of miR-193b are involved in signaling pathways such as MAP3K3, WNT, P53, Jak-STAT, GnRH, VEGF, ErbB, angiogenesis, cell cycle G1/S check point, cell motility and adherens junction, which are important for tumorigenesis (*Figure 4A*).

miR-193b down-regulated uPA protein in GC cells

We were interested in oncogenes potentially inhibited by miR-193b and uPA attracted our attention. Western blot demonstrated that uPA protein was up-regulated upon miR-193b inhibition and down-regulated upon miR-193b mimic (*Figure 4B*). qRT-PCR showed no significant uPA mRNA changes upon miR-193b inhibition or mimic (*Figure 4C*).
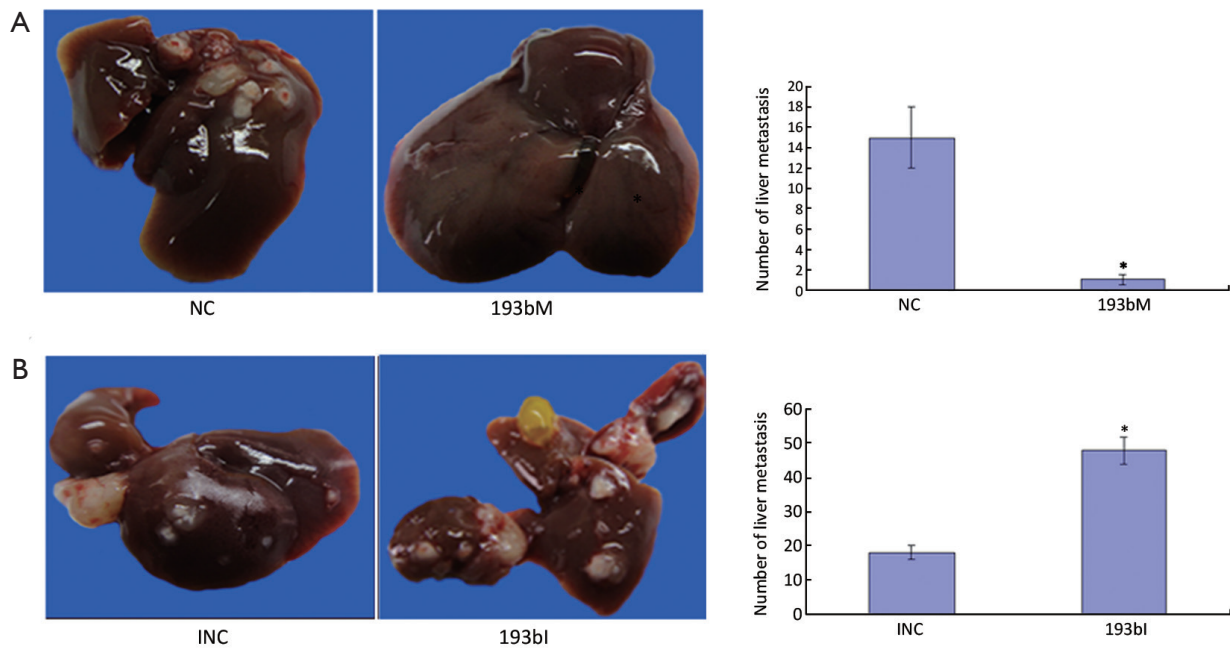
Figure 3 *In vivo* metastasis assay. BGC823 cells transfected with 193b mimics or inhibitors were injected into abdominal cavity of nude mice. A. Representative photos of lives from mice injected with BGC823-193b mimics or BGC823-NC (n=6). *P<0.05; B. Representative photos of lives from mice injected with BGC823-193b inhibitor or BGC823-INC (n=6). *P<0.05. NC, negative control for BGC823-193b mimics; 193bM, BGC823-193b mimics; INC, negative control for BGC823-193b inhibitor; 193bI, BGC823-193b inhibitor
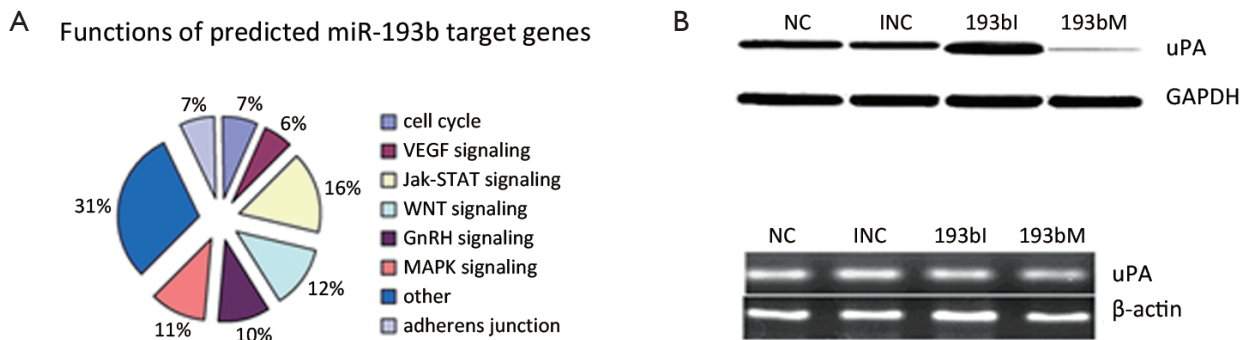

Figure 4 miR-193b down-regulated uPA protein in GC cells. A. Pie chart of predicted target genes involved in different pathways analyzed by Functional Annotation Bioinformatics Microarray Analysis Tools from CapitalBio Corporation; B. uPA protein expression levels were increased upon transfection with 193bI and decreased upon transfection with 193bM compared with control; C. uPA mRNA levels have no significant changes upon transfection with 193bI or 193bM compared with control. NC, negative control for BGC823-193b mimics; 193bM, BGC823-193b mimics; INC, negative control for BGC823-193b inhibitor; 193bI, BGC823-193b inhibitor

Discussion

Increasing evidence indicates that the TGF-β signaling pathway may be regulated by several miRNAs, such as miR-23a, miR-17-92 and miR-155 (14-19). In this study, we discovered six differentially expressed miRNAs (miR-193b, miR-574-3p, miR-130b, miR-27a, miR-29b-1 and miR-194) in BGC823 cells using microRNA microarrays upon TGF-β1 stimulation. All of these miRNAs are regarded as tumor-related miRNAs (20-27) and relevant to invasion and metastasis of GC. In our previous study, we observed

high expression of TGF-β type II Ser/Thr receptor in BGC823, SGC7901 and MKN28 cells (28). BGC823 and SGC7901 were sensitive to TGF-β (29,30), while MKN28 was resistant, which might be attributed to low binding activity of type-I receptor of TGF-β (31) or mutation of RUN-X3 (32). We further confirmed by real-time PCR that disregulation of three miRNAs was coincident with miRNA microarray after TGF-β1 pretreatment both in BGC823 and SGC7901, but there was no visible change in MKN28. Meanwhile, BGC823 is a kind of cell with poor differentiation, which is more representative. So, we most used this kind of cells in this research. These results indicated that the changes of these miRNAs may be regulated by the TGF-β pathway.

Among the miRNAs studies, miR-193b exhibited the most dramatic downregulation, and miR-193b was therefore selected for further study. miR-193b targets cyclin D1 (33) in melanoma, repressing cell proliferation. Xu *et al.* (34) found that miR-193b regulated oncogenes cyclin D1 (CCND1) and ETS1, and induced cell cycle arrest and inhibited the invasion and migration of hepatoma cells. Li *et al.* (35) found that the down-regulation of miR-193b enhanced uPA expression, and promoted tumor progression and invasion in human breast cancer. However, two genes, CCND1 and ETS1, whether they are still direct target of miR-193b in GC cell lines is unclear. At present, we are revealing the relation between them. In this study, we found that the over-expression of miR-193b reduced the capacity of migration, invasion and metastasis of the GC cell BGC823 *in vivo* and *in vitro*.

uPA is a serine protease responsible for the conversion of plasminogen into plasmin. It plays a major role in regulating cancer cell motility, extracellular matrix invasion and metastasis by degrading extracellular matrix proteins (36,37). Overexpression of uPA is directly associated with tumor growth, invasion and metastasis (38-41). In addition, uPA expression and activity are positively correlated with infiltration, metastasis and peritoneal metastasis in GC (42). Interestingly, there is a binding site for hsa-miR-193b in uPA 3'-UTR that has been experimentally verified to be active in human breast cancer. In addition, we infer miR-193b may be influence the uPA translation rather than transcription (43). In our study, uPA protein was up-regulated upon miR-193b inhibition and down-regulated upon miR-193b mimic, but no uPA mRNA change was seen upon miR-193b inhibition or mimic. miR-193b down-regulated uPA protein in GC cells. However, the specific relation between the uPA and miR-193b was unclear. At present, the relation research is performing by siRNA methods.

Our finding shed light on the following questions: Is the dysregulation of miR-193b through TGF-β pathway? Is uPA a direct target of miR-193b? Does miR-193b inhibit the invasion and metastasis of BGC823 cells by down-regulating uPA? TGF-β, miRNAs and genes may constitute a gene-miRNA network to contribute to GC progression. Further research is necessary to completely answer the puzzles. At present, we use miR-193b as a therapy target to find out specific effect for downstream pathway. In addition, the research that therapeutic delivery of miR-193b suppresses tumorigenesis in GC mouse model is being performed.

In conclusion, our study demonstrated that TGF-β1 leads to a specific alternation of miRNA profile in BGC823 cell line. TGF-β1 induces the down-regulation of miR-193b in BGC823 and SGC7901 cell lines. miR-193b inhibits cell migration and invasion *in vitro*, as well as tumor invasion and metastasis *in vivo*. miR-193b down-regulates uPA protein in GC cells.

Acknowledgements

References

1. Herszényi L, Tulassay Z. Epidemiology of gastrointestinal and liver tumors. Eur Rev Med Pharmacol Sci 2010;14:249-58.
2. Kloosterman WP, Plasterk RH. The diverse functions of microRNAs in animal development and disease. Dev Cell 2006;11:441-50.
3. Esquela-Kerscher A, Slack FJ. Oncomirs - microRNAs with a role in cancer. Nat Rev Cancer 2006;6:259-69.
4. Lu J, Getz G, Miska EA, et al. MicroRNA expression profiles classify human cancers. Nature 2005;435:834-8.
5. Derynck R, Akhurst RJ. Differentiation plasticity regulated by TGF-beta family proteins in development and disease. Nat Cell Biol 2007;9:1000-4.
6. Annes JP, Munger JS, Rifkin DB. Making sense of latent TGFbeta activation. J Cell Sci 2003;116:217-24.
7. Park D 2nd, Son HJ, Song SY, et al. Role of TGF-beta 1 and TGF-beta type II receptor in gastric cancer. Korean J Intern Med 2002;17:160-6.
8. Kuwahara A, Katano M, Nakamura M, et al. New

therapeutic strategy for gastric carcinoma: a two-step evaluation of malignant potential from its molecular biologic and pathologic characteristics. J Surg Oncol 1999;72:142-9.

9. Wang KS, Hu ZL, Li JH, et al. Enhancement of metastatic and invasive capacity of gastric cancer cells by transforming growth factor-beta1. Acta Biochim Biophys Sin (Shanghai) 2006;38:179-86.

10. Kong W, Yang H, He L, et al. MicroRNA-155 is regulated by the transforming growth factor beta/Smad pathway and contributes to epithelial cell plasticity by targeting RhoA. Mol Cell Biol 2008;28:6773-84.

11. Davis BN, Hilyard AC, Lagna G, et al. SMAD proteins control DROSHA-mediated microRNA maturation. Nature 2008;454:56-61.

12. Hwang HW, Mendell JT. MicroRNAs in cell proliferation, cell death, and tumorigenesis. Br J Cancer 2006;94:776-80.

13. Ma L, Weinberg RA. Micromanagers of malignancy: role of microRNAs in regulating metastasis. Trends Genet 2008;24:448-56.

14. Wang B, Hsu SH, Majumder S, et al. TGFbeta-mediated upregulation of hepatic miR-181b promotes hepatocarcinogenesis by targeting TIMP3. Oncogene 2010;29:1787-97.

15. Rai D, Kim SW, McKeller MR, et al. Targeting of SMAD5 links microRNA-155 to the TGF-beta pathway and lymphomagenesis. Proc Natl Acad Sci U S A 2010;107:3111-6.

16. Zhang L, Deng T, Li X, et al. MicroRNA-141 is involved in a nasopharyngeal carcinoma-related genes network. Carcinogenesis 2010;31:559-66.

17. Cho JH, Gelinas R, Wang K, et al. Systems biology of interstitial lung diseases: integration of mRNA and microRNA expression changes. BMC Med Genomics 2011;4:8.

18. Mestdagh P, Boström AK, Impens F, et al. The miR-17-92 microRNA cluster regulates multiple components of the TGF-β pathway in neuroblastoma. Mol Cell 2010;40:762-73.

19. Louafi F, Martinez-Nunez RT, Sanchez-Elsner T. MicroRNA-155 targets SMAD2 and modulates the response of macrophages to transforming growth factor-{beta}. J Biol Chem 2010;285:41328-36.

20. Gui J, Tian Y, Wen X, et al. Serum microRNA characterization identifies miR-885-5p as a potential marker for detecting liver pathologies. Clin Sci (Lond) 2011;120:183-93.

21. Wang W, Peng B, Wang D, et al. Human tumor MicroRNA signatures derived from large-scale oligonucleotide microarray datasets. Int J Cancer 2011;129:1624-34.

22. Yeung ML, Yasunaga J, Bennasser Y, et al. Roles for microRNAs, miR-93 and miR-130b, and tumor protein 53-induced nuclear protein 1 tumor suppressor in cell growth dysregulation by human T-cell lymphotrophic virus 1. Cancer Res 2008;68:8976-85.

23. Malzkorn B, Wolter M, Liesenberg F, et al. Identification and functional characterization of microRNAs involved in the malignant progression of gliomas. Brain Pathol 2010;20:539-50.

24. Lai KW, Koh KX, Loh M, et al. MicroRNA-130b regulates the tumour suppressor RUNX3 in gastric cancer. Eur J Cancer 2010;46:1456-63.

25. Su X, Chakravarti D, Cho MS, et al. TAp63 suppresses metastasis through coordinate regulation of Dicer and miRNAs. Nature 2010;467:986-90.

26. Steele R, Mott JL, Ray RB. MBP-1 upregulates miR-29b that represses Mcl-1, collagens, and matrix-metalloproteinase-2 in prostate cancer cells. Genes Cancer 2010;1:381-7.

27. Meng Z, Fu X, Chen X, et al. miR-194 is a marker of hepatic epithelial cells and suppresses metastasis of liver cancer cells in mice. Hepatology 2010;52:2148-57.

28. Zhang Y, Fan KJ, Sun Q, et al. Functional screening for miRNAs targeting Smad4 identified miR-199a as a negative regulator of TGF-β signalling pathway. Nucleic Acids Res 2012;40:9286-97.

29. Hu ZL, Wen JF, Xiao DS, et al. Effects of transforming growth interacting factor on biological behaviors of gastric carcinoma cells. World J Gastroenterol 2005;11:84-8.

30. Li X, Zhang YY, Wang Q, et al. Association between endogenous gene expression and growth regulation induced by TGF-beta 1 in human gastric cancer cells. World J Gastroenterol 2005;11:61-8.

31. Li QL, Ito K, Sakakura C, et al. Causal relationship between the loss of RUNX3 expression and gastric cancer. Cell 2002;109:113-24.

32. Kong W, Yang H, He L, et al. MicroRNA-155 is regulated by the transforming growth factor beta/Smad pathway and contributes to epithelial cell plasticity by targeting RhoA. Mol Cell Biol 2008;28:6773-84.

33. Chen J, Feilotter HE, Paré GC, et al. MicroRNA-193b represses cell proliferation and regulates cyclin D1 in melanoma. Am J Pathol 2010;176:2520-9.

34. Xu C, Liu S, Fu H, et al. MicroRNA-193b regulates proliferation, migration and invasion in human hepatocellular carcinoma cells. Eur J Cancer 2010;46:2828-36.

35. Li XF, Yan PJ, Shao ZM. Downregulation of miR-193b contributes to enhance urokinase-type plasminogen activator (uPA) expression and tumor progression and invasion in human breast cancer. Oncogene 2009;28:3937-48.

36. Dorn J, Harbeck N, Kates R, et al. Impact of expression differences of kallikrein-related peptidases and of uPA and PAI-1 between primary tumor and omentum metastasis in advanced ovarian cancer. Ann Oncol 2011;22:877-83.

37. Märkl B, Renk I, Oruzio DV, et al. Tumour budding, uPA and PAI-1 are associated with aggressive behaviour in colon cancer. J Surg Oncol 2010;102:235-41.

38. Huang HY, Jiang ZF, Li QX, et al. Inhibition of human breast cancer cell invasion by siRNA against urokinase-type plasminogen activator. Cancer Invest 2010;28:689-97.

39. Achbarou A, Kaiser S, Tremblay G, et al. Urokinase overproduction results in increased skeletal metastasis by prostate cancer cells in vivo. Cancer Res 1994;54:2372-7.

40. Sliva D, Rizzo MT, English D. Phosphatidylinositol 3-kinase and NF-kappaB regulate motility of invasive MDA-MB-231 human breast cancer cells by the secretion of urokinase-type plasminogen activator. J Biol Chem 2002;277:3150-7.

41. Pakneshan P, Szyf M, Farias-Eisner R, et al. Reversal of the hypomethylation status of urokinase (uPA) promoterblocks breast cancer growth and metastasis. J Biol Chem 2004;279:31735-44.

42. Pulukuri SM, Rao JS. Small interfering RNA directed reversal of urokinase plasminogen activator demethylation inhibits prostate tumor growth and metastasis. Cancer Res 2007;67:6637-46.

43. Ding YC, Zhu ZG, Liu BY, et al. Relationship between urokinase-type plasminogen activator expression and peritoneal metastatic potency in different gastric cancer cell lines. Zhonghua Wei Chang Wai Ke Za Zhi 2005;8:249-51.